



In Vitro and *In Vivo* Trypanocidal Activity of H₂bdtc-Loaded Solid Lipid Nanoparticles

Zumira A. Carneiro¹, Pedro I. da S. Maia², Renata Sesti-Costa³, Carla D. Lopes³, Tatiana A. Pereira¹, Cristiane M. Milanezi³, Marcelo A. Pereira da Silva^{4,5}, Renata F. V. Lopez¹, João S. Silva³, Victor M. Deflon^{2*}

1 Faculdade de Ciências Farmacêuticas de Ribeirão Preto, University of São Paulo, Ribeirão Preto, São Paulo, Brazil, **2** Instituto de Química de São Carlos, University of São Paulo, São Carlos, São Paulo, Brazil, **3** Departamento de Bioquímica e Imunologia, School of Medicine, University of São Paulo, Ribeirão Preto, São Paulo, Brazil, **4** Instituto de Física de São Carlos, University of São Paulo, São Carlos, São Paulo, Brazil, **5** Centro Universitário Central Paulista - UNICEP, São Carlos, São Paulo, Brazil

Abstract

The parasite *Trypanosoma cruzi* causes Chagas disease, which remains a serious public health concern and continues to victimize thousands of people, primarily in the poorest regions of Latin America. In the search for new therapeutic drugs against *T. cruzi*, here we have evaluated both the *in vitro* and the *in vivo* activity of 5-hydroxy-3-methyl-5-phenyl-pyrazoline-1-(*S*-benzyl dithiocarbamate) (H₂bdtc) as a free compound or encapsulated into solid lipid nanoparticles (SLN); we compared the results with those achieved by using the currently employed drug, benznidazole. H₂bdtc encapsulated into solid lipid nanoparticles (a) effectively reduced parasitemia in mice at concentrations 100 times lower than that normally employed for benznidazole (clinically applied at a concentration of 400 μmol kg⁻¹ day⁻¹); (b) diminished inflammation and lesions of the liver and heart; and (c) resulted in 100% survival of mice infected with *T. cruzi*. Therefore, H₂bdtc is a potent trypanocidal agent.

Citation: Carneiro ZA, Maia PIdS, Sesti-Costa R, Lopes CD, Pereira TA, et al. (2014) *In Vitro* and *In Vivo* Trypanocidal Activity of H₂bdtc-Loaded Solid Lipid Nanoparticles. PLoS Negl Trop Dis 8(5): e2847. doi:10.1371/journal.pntd.0002847

Editor: Michael P. Pollastri, Northeastern University, United States of America

Received: November 10, 2013; **Accepted:** March 25, 2014; **Published:** May 8, 2014

Copyright: © 2014 Carneiro et al. This is an open-access article distributed under the terms of the Creative Commons Attribution License, which permits unrestricted use, distribution, and reproduction in any medium, provided the original author and source are credited.

Funding: This work was supported by the Research Foundation of the State of São Paulo (FAPESP 2010/20610-0). The funders had no role in study design, data collection and analysis, decision to publish, or preparation of the manuscript.

Competing Interests: The authors have declared that no competing interests exist.

* E-mail: deflon@iqsc.usp.br

Introduction

T. cruzi parasites are transmitted by insect vectors (triatomine bugs). *T. cruzi* is the causative agent of Chagas disease, which is silent and can remain asymptomatic for years [1], [2], [3]. A century after its discovery, this disease remains a serious public health issue—it is closely associated with human poverty and political instability as well as with little investment in drug development. According to the World Health Organization (WHO), between seven and eight million people are infected with *T. cruzi* worldwide, primarily in Latin America [4], [5], [6]. One in every four Chagas patients develops a fatal symptom of the disease due to lack of adequate diagnosis and treatment.

Nifurtimox and benznidazole (BZN) are currently available to treat the disease [7], [8], [9], [10]. However, neurological side effects have led commercial nifurtimox production to be discontinued [11]. As for BZN, although it is mainly effective during the acute phase of the infection, it presents undesirable side effects such as rash and gastrointestinal symptoms [12], so patients often fail to comply with the treatment [8]. Long treatment periods (30, 60, or 90 days) and appropriate pediatric formulations not available (administration of the medication to children often requires tablet fractionation) also limit BZN use [9], [11], [13]. A further concern is that no effective treatment for the symptomatic chronic phase of Chagas disease exists, so the patients usually receive palliative drugs at this stage [14], [15]. Therefore, a

number of researchers are making considerable efforts to find new drugs to combat this disease.

Dithiocarbazates display notable biological and pharmacological properties, including anticancer [16], [17], antimicrobial [17], [18], [19], and insecticidal activities [20]. A recent study has shown that cyclic compounds derived from *S*-dithiocarbamate and 1,3-diketones exhibit significant trypanocidal activity [21]: in particular, 5-hydroxy-3-methyl-5-phenyl-pyrazoline-1-(*S*-benzyl-dithiocarbamate) (previously referred to as H₂L^{2a} [21]) which was renamed H₂bdtc in this reference in this work (Figure 1) constitutes a potential drug lead to develop a new agent against the trypomastigote form of Tulahuen strains of *T. cruzi* [21]. Nevertheless, the lipophilic character of H₂bdtc may limit its administration and result in low oral bioavailability [22].

Drug delivery systems can help to circumvent this problem. Because lipids have excellent physiological acceptability and can promote drug absorption as well as selective lymphatic uptake, researchers have focused on lipid-based drug release systems [23]. In particular, solid lipids constitute solid lipid nanoparticles (SLNs) at room and body temperature. Since SLNs consist of biocompatible and biodegradable lipids with low or no human toxicity, they can function as drug delivery systems [24], [25]. SLNs offer many advantages: they protect the drug against degradation, enable controlled drug release, and dismiss the use of organic solvents. Moreover, SLNs can be produced on a large scale, meeting industrial requirements [24], [26].

Author Summary

The protozoan parasite *Trypanosoma cruzi* causes Chagas disease, a condition that affects the poorest regions of Latin America mainly. The chronic phase of this disease disables thousands of patients, constituting an important public health issue. The pharmacotherapy that is currently applied to treat the disease emerged many decades ago, is ineffective in most patients, mainly during the chronic phase, and has serious side effects. In a recent study, we showed that the compound 5-hydroxy-3-methyl-5-phenylpyrazoline-1-(S-benzyl)dithiocarbamate (H₂bdtc) is a potential drug candidate against the *in vitro* trypomastigote form of Tulahuen strains of *T. cruzi*. Here we report that H₂bdtc loaded into solid lipid nanoparticles (H₂bdtc-SLNs) displays good trypanocidal activity against the trypomastigote form of the Y strain of *T. cruzi* both *in vitro* and *in vivo*. Our *in vivo* experiments revealed that H₂bdtc-SLN is 100 times more active than benznidazole (BZN), the drug that is commercially available to treat Chagas disease. Surprisingly, this compound has no side effects on the *T. cruzi* acute phase. Hence, we propose that H₂bdtc-SLNs possesses interesting anti-*Trypanosoma* properties.

Our group has used H₂bdtc *in vitro* experiments involving the Tulahuen strain (group I) [21]. The resistances of this group and of the Y strain (group II) have been reported to be different, based on phosphatase activities in *T. cruzi* homogenates [27]. Tulahuen had an optimum phosphatase activity at pH 4.0 and the Y strain at pH 7.0 [27]. Also in chronic phase has been associated with *T. cruzi* II-restricted infections [28]. In this sense, evaluating the trypanocidal activity of H₂bdtc against the Y strain could support the use of this compound as a new drug against *T. cruzi*. In addition, so far little attention has been paid to the use of SLNs to treat Chagas disease [29], [30]. Therefore, this work investigates the *in vitro* and *in vivo* trypanocidal activity of free H₂bdtc and H₂bdtc encapsulated into SLNs (H₂bdtc-SLNs) against the Y strain of *T. cruzi* and compares results with data obtained for the currently available drug BZN.

Materials and Methods

General

BZN, a product manufactured by Lafepe, Brazil, was used as a reference drug. The synthesis of H₂bdtc has been described previously [21]. RPMI Medium 1640 supplemented with 5% bovine fetal serum (GIBCO, Grand Island, NY, USA), 100 IU mL⁻¹ penicillin G, and 100 mg mL⁻¹ streptomycin (Gibco-BRL, Grand Island, NY, USA) was employed. Dimethyl sulfoxide (DMSO) and propidium iodide (PI) were obtained from Sigma-Aldrich Chemicals Co. (St. Louis, MO, USA). Stearic acid and sodium taurodeoxycholate were purchased from Sigma-Aldrich (St. Louis, MO, USA), Lipoid S 100 (soya lecithin) was acquired from Lipoid (Ludwigshafen, KOLN, Germany), and Amicon Ultra 15, MWCO 100 K, was provided by Millipore (Billerica, MA, USA).

Preparation of H₂bdtc-loaded solid lipid nanoparticles (H₂bdtc-SLNs)

SLNs were prepared using a microemulsion method [31]. Briefly, the desired amount of sodium taurodeoxycholate (0.12% w/v) was dissolved in hot aqueous phase, which was added to melted stearic acid (0.95% w/v) containing soya lecithin (0.48% w/v) and H₂bdtc (0.02% w/v). The mixture was emulsified with

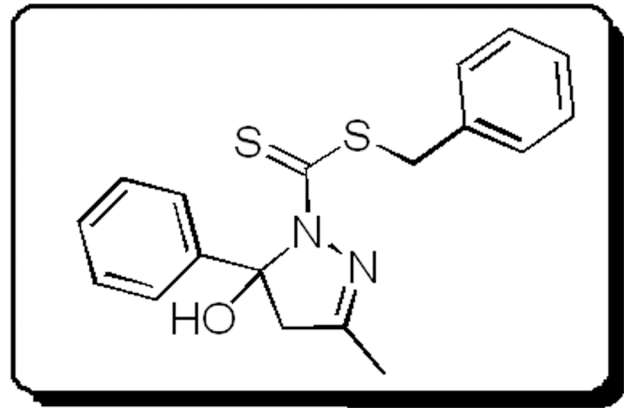


Figure 1. General molecular structure of the new cyclic S-dithiocarbamate derivatives.

doi:10.1371/journal.pntd.0002847.g001

magnetic stirring at $90.0 \pm 2.0^\circ\text{C}$, until a thermodynamically stable microemulsion formed. The SLNs dispersion was obtained by cooling the hot microemulsion in cold water ($2\text{--}5^\circ\text{C}$) under vigorous stirring at 20,000 rpm for 10 min (IKA-T25 Ultra-turrax, Germany) at 1:20 ratio (microemulsion/cold water). Next, the SLNs aqueous dispersion was subjected to high-pressure homogenization (EmulsiFlex – C3, Germany) at 500 bars for 10 min.

Particle size, dispersity index (D-stroke), and zeta potential determination

The particle size and dispersity of the H₂bdtc-SLNs dispersion were measured via photon correlation spectroscopy (PCS) [32]; the zeta potential was determined on the basis of the electrophoresis mobility of the nanoparticles using the Zetasizer ZS Nano 90 (Malvern Instruments, UK.). The samples were diluted (1:10) with distilled water at 25.0°C .

Atomic Force Microscopy (AFM)

The morphology of H₂bdtc-SLNs was assessed using an atomic force microscope (ICON Bruker, USA). The samples were prepared by immersing freshly cleaved mica (Muscovite Mica Substrates Sheets, SPI Supplies, China) in SLNs aqueous dispersion and stored overnight, at room temperature, to complete the drying process. The samples were evaluated by AFM in the intermittent contact mode (tapping mode) by scanning the surface of mica ($2\ \mu\text{m} \times 2\ \mu\text{m}$ in area) using a rectangular silicon cantilever with a spring constant of $40\ \text{N m}^{-1}$ vibrating at a frequency of 320 kHz. Imaging was performed at room temperature, and the topology image was used to determine the morphology of H₂bdtc-SLNs [33].

Drug entrapment efficiency (EE%) determination

The total H₂bdtc content in the H₂bdtc-SLNs was determined by UV-vis spectroscopy at 400 nm (UV Spectrophotometer UV 1800, Shimadzu, Japan). First, a defined amount of H₂bdtc-SLNs was dissolved in dimethyl sulfoxide. The amount of encapsulated drug was indirectly measured after centrifuging the H₂bdtc-loaded SLNs for 40 min at 6000 rpm (1605 G), at 25°C in a centrifuge (Heraeus Megafuge 16 R Thermo Scientific, USA) equipped with a membrane concentrator (Amicon Ultra 15, MWCO 100 K, Millipore Corporation, USA). The filtrate was diluted with dimethyl sulfoxide (1:1), and the concentration of free H₂bdtc in

the diluted filtrate was determined using the same conditions employed to measure the total H₂bdtc content used during the loading procedure (section 2.2). The amount of H₂bdtc loaded into SLNs was calculated by subtracting the amount of free H₂bdtc in the filtrate from the total amount of H₂bdtc used during loading (26). EE (%) was determined using the following equation [26], [34].

$$EE\% = \frac{\text{drug loading}}{\text{theoretical drug loading}} \times 100$$

Partition coefficient of H₂bdtc ($K_{\text{octanol/water}}$)

Partition coefficients for the H₂bdtc were determined in triplicate in an n-octanol/water system following a published procedure [35]. Measurements of H₂bdtc n-octanol/water partition coefficients were carried out using the shake-flask method. H₂bdtc was dissolved in aqueous solution previously saturated with n-octanol at a concentration of 1 mg/mL and mixed with the same volume of octanol also previously saturated with water. Samples were stirred for 30 min, separate in two phases, and centrifuged for 10 min at 2000 rpm. The amount of H₂bdtc in the aqueous phase was quantified by UV-visible spectroscopy.

Mice

Female Swiss mice (6 to 8 weeks old) were bred and maintained at the Department of Biochemistry and Immunology, School of Medicine of Ribeirao Preto, University of São Paulo, Ribeirão Preto, Brazil. The mice were maintained in microisolator cages under standard conditions; they were fed with food and water ad libitum.

Ethics statement

All the *in vivo* procedures were performed in accordance with the guidelines issued by the Brazilian College of Animal experimentation (COBEA) and received prior approval by the Ethics Committee on Animal Experimentation – CETEA (n° 006/2011) of the School of Medicine of Ribeirão Preto.”

Parasites and experimental infection

All the experiments were conducted using the trypomastigote form of the Y strain of *T. cruzi* (Lineage type II). For the *in vitro* experiments, parasites were grown in a fibroblast cell line (LLC-MK2). For the *in vivo* experiments, mice were intraperitoneally inoculated with 2.0×10^3 bloodstream trypomastigote forms, which had been derived from previously infected Swiss mice.

In vitro evaluation of the trypanocidal activity and cytotoxicity of free H₂bdtc and H₂bdtc-loaded SLNs

The trypanocidal activities of free H₂bdtc, H₂bdtc-SLNs, and BZN against the trypomastigote form of the *T. cruzi* Y strains were evaluated as described previously [36]. To this end, the trypomastigote culture at a concentration of 6.5×10^6 parasites mL⁻¹ was re-suspended in RPMI 1640 medium with 5% FBS. Triplicate cultures were treated with one of the investigated drugs and maintained at $37.0 \pm 0.1^\circ\text{C}$ in a humidified atmosphere of 5% CO₂. To test parasite viability, the number of motile forms was determined using a previously described method [37]. The concentration of compound corresponding to 50% trypanocidal activity after 24 h of incubation was expressed as the IC_{50try} (inhibitory concentration for the trypomastigote form).

Spleen cells isolated from C57BL/6 mice, macerated in RPMI 1640 medium (Gibco), and filtered using a 100- μm pore filter were used to evaluate the cytotoxicity *in vitro*. The isolated cells were centrifuged at 1500 rpm for 10 min, and erythrocytes were lysed in lysis buffer for 5 min, at room temperature. Cells were washed, counted, and resuspended at 6.5×10^6 mL⁻¹ in RPMI medium containing 5% fetal bovine serum. The spleen cells were seeded to a 96-well microplate (n = 2) and incubated for 24 h with H₂bdtc diluted in dimethyl sulfoxide (DMSO, final H₂bdtc concentration not exceeding 0.5%) or H₂bdtc-SLNs (concentrations ranging from 125 μM to 0.24 μM in serial dilutions). BZN (Roche) was used as the reference drug; Tween 20 was employed as positive control for cell death. After the incubation period, the cells were washed and incubated with propidium iodide at a final concentration of 10 $\mu\text{g mL}^{-1}$. Cell cytotoxicity was measured on a flow cytometer (FACSCantoII - BD), and the data were analyzed using the FlowJo program (Tree Star).

In vivo evaluation of the cytotoxicity and trypanocidal activity of free H₂bdtc and H₂bdtc-SLNs

Female Swiss mice aged between 6 and 8 weeks, weighing between 20 and 25 g, were infected with 2.0×10^3 blood trypomastigotes per animal. A total of four experimental groups consisting of seven Swiss mice each were included in the study. Treatment started at day 5 post-inoculation (p.i.). BZN, free H₂bdtc and H₂bdtc-SLNs were orally administered at 4 $\mu\text{mol kg}^{-1}$ (BZN 1.0 mg kg⁻¹ day⁻¹/free H₂bdtc and H₂bdtc-SLNs 1.4 mg kg⁻¹ day⁻¹) per day for 10 consecutive days. The following treatments were applied: Group 1 = PBS control group; infected and not treated, Group 2 = infected and treated with BZN, Group 3 = infected and treated with free H₂bdtc, and Group 4 = infected and treated with H₂bdtc-SLNs. To evaluate parasitaemia and mortality, seven animals from each group were used. Seven animals were killed at day 22 p.i. (early mortality), to quantify inflammation of the heart and liver and to measure creatine kinase-MB (CK-MB) and glutamic-pyruvic transaminase (GPT) production.

Parasitemia and mortality

Parasitemia was analyzed on alternate days from day 7 p.i.; to this end, 5 μL of fresh blood was collected from the animal tail. The count of 100 fields was performed via direct observation under a light microscope [38]. Mortality was inspected on a daily basis until day 60.

Histological analysis

Groups of seven mice were euthanized at day 20 p.i., and portions of the heart and liver were fixed in paraffin for histological analysis. To assess inflammatory infiltration via light microscopy DP71 (Olympus Optical Co, Japan), tissues were sectioned at a 5- μm thickness and stained with hematoxylin-eosin (H&E). Each tissue section was imaged 25 times, and the percentage of the area occupied by cellular infiltrates was determined using the Image J program.

Quantitative real-time PCR (qPCR)

Quantitative PCR was used to determine the amount of parasitic DNA in heart tissues. Briefly, DNA was purified from 25 mg of heart tissue using a QIAamp DNA Mini Kit (Qiagen), according to the manufacturer's instructions. Each PCR reaction comprised 40 ng of genomic DNA; 0.3 μM of the *T. cruzi*-specific primers TCZ-F 5'-GCTCTTGCCACAMGGGTGC-3' (M = A or C) TCZ-R 5'-CCAAGCAGCGGATAGTTCAGG-3' [39],

Table 1. Particle size, zeta potential, dispersity index and entrapment efficiency of SLNs (mean \pm SD, n=3).

Formulation				
Compounds	Mean Particle (nm)	D-Stroke	Zeta Potential (mV)	Entrapment Efficiency (%)
SLN	132.3 \pm 10.2	0.260 \pm 0.0098	-60.20 \pm 2.30	98.16 \pm 1.12
H ₂ bdtc-SLN	127.4 \pm 0.130	0.229 \pm 0.130	-56.10 \pm 4.40	

*Dispersity (D-stroke). SLNs: SLNs without drug loaded and H2bdtc loaded in SLNs; H2bdtc loaded in SLNs.
doi:10.1371/journal.pntd.0002847.t001

which amplify a 182-bp product; 7.65 μ L of GoTaq qPCR Master Mix; and H₂O (final total volume of 15 μ L).

The reactions were performed using the Real-Time PCR System. The cycling program involved a denaturation cycle of 95.0°C for 10 min, followed by 40 cycles of the three steps of the amplification phase: 95.0°C for 15 s, 55.0°C for 30 s, and 72.0°C for 15 s. The melting phase was performed at 95.0°C for 15 s and at 60.0°C for 1 min, followed by a 0.3°C ramp and then 95.0°C for 15 s. During the melting phase, the acquisition setting was set at step. The data were analyzed with StepOne Software version 2.2.2.

Serum activity of creatine kinase isoform MB (CK-MB) and glutamic-pyruvic transaminase (GPT)

The cardiac and hepatic lesions of mice infected with *T. cruzi*, treated or not, were assessed by measuring the creatine kinase-MB (CK-MB) and glutamic-pyruvic transaminase (GPT) levels, respectively, in the serum at day 22 p.i. The CK-MB levels were measured using a CK-MB kit (Liquiform, Brazil), as previously described [40]. Absorbance was measured on a microplate spectrophotometer (EMAX Molecular Devices Corporation, California, EUA). The color produced from this reaction was measured at a wavelength of 340 nm; the results are expressed in U/I. GPT was analyzed using an ALT/GPT kit (Liquiform, Brazil), according to the manufacturer's instructions. The colorimetric assay determines the amount of pyruvate produced according to the Reitman and Frankel method, from the

formation of 2,4-dinitrophenylhydrazine [41]. The color produced by this reaction was measured at a wavelength of 505 nm.

Statistical analyses

Data are expressed as the mean SEM. Student's t-test was used to analyze the statistical significance of the variation between the infected and control assays. Differences were considered statistically significant when $P < 0.05$. The differences in droplet size, dispersity, zeta potential, and entrapment efficiency values achieved during the stability test were evaluated via a one-way ANOVA analysis of variance followed by Tukey post-test analysis. The differences were considered statistically significant when $P < 0.05$. All the analyses were performed using PRISM 5.0 software (Graph Pad, San Diego, CA, US).

Results

Preparation and characterization of H₂bdtc-SLNs

The H₂bdtc showed a lipophilic character (Log P (o/w) = 2.69 \pm 0.03) and were efficiently encapsulated in this manner in SLNs. On the basis of Photon Correlation Spectroscopy (PCS), H₂bdtc-SLNs had diameter of 127.4 \pm 10.2 nm and dispersity lower than 0.3; the zeta potential revealed a negative surface charge (-56.1 \pm 4.4 mV) (Table 1). The entrapment efficiency was 98.16 \pm 1.12, showing that the drug dispersed well within the lipid matrix. Atomic force microscopy images revealed that

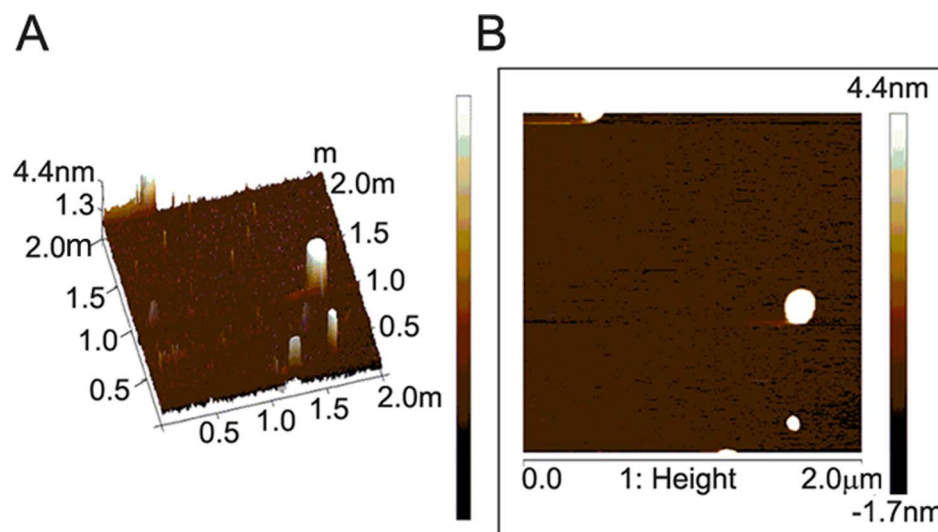


Figure 2. Atomic Force Microscopy micrographs of H₂bdtc loaded in SLNs (A) 2 μ m \times 2 μ m three-dimensional image. (B) 2 μ m \times 2 μ m planar image.

doi:10.1371/journal.pntd.0002847.g002

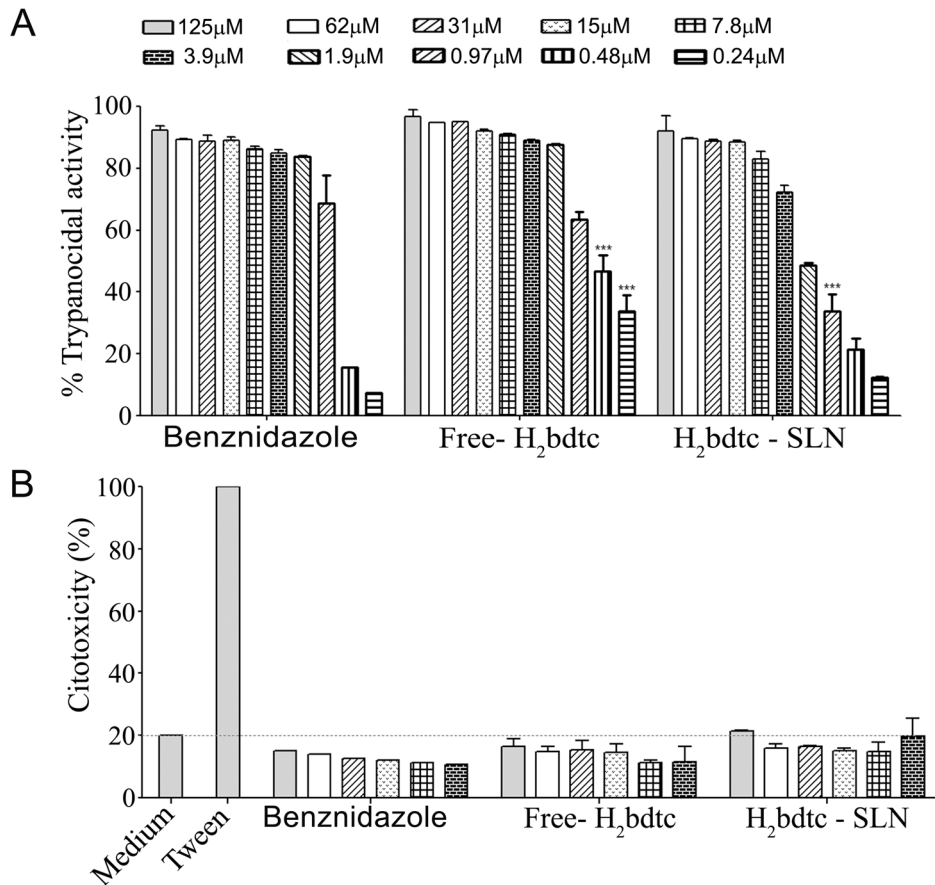


Figure 3. *In vitro* evaluation of the trypanocidal activity and cytotoxicity of H₂bdtc – (concentrations range from 125 μM to 0.24 μM in serial dilutions). (A) Percentage of trypanocidal activity of free H₂bdtc and H₂bdtc loaded in SLNs against the Y strain of *T. cruzi* analyzed by quantifying viable parasites via microscopy after 24 h post-treatment. (B) Percentage of cytotoxicity of free H₂bdtc and H₂bdtc loaded in SLNs in spleen cells derived from mice after 24 h via propidium iodide treatment and FACS analysis. The mean + SEM is shown and is representative of three independent experiments (n = 2). Statistically significant differences compared with the control (BZN). Anova, Bonferroni post - test: ***p<0.001 doi:10.1371/journal.pntd.0002847.g003

H₂bdtc-SLNs particles were spherical, with an average diameter of approximately 180 nm (Figure 2), agreeing with the PCS results.

In vitro evaluation of the trypanocidal activity and cytotoxicity of free H₂bdtc and H₂bdtc- SLNs

We assessed the *in vitro* trypanocidal activity of free H₂bdtc, H₂bdtc-SLNs and BZN after 24 h of incubation with *T. cruzi* trypomastigotes forms. Free H₂bdtc presents IC_{50try} (inhibitory concentrations against bloodstream trypomastigote) as 0.50±0.12, H₂bdtc-SLNs as 1.83±0.18 and BZN 0.50±0.39 μM (Figure 3A). We also measured the cytotoxicity of free H₂bdtc and H₂bdtc-SLNs in spleen cells of Swiss mice; none of the tested drugs was significantly cytotoxic (Figure 3B). Hence, both free H₂bdtc and H₂bdtc-SLNs displayed similar *in vitro* trypanocidal activity to BZN; this activity was not associated with general cytotoxicity but rather with specific activity against the parasite.

In vivo activity of free H₂bdtc and H₂bdtc-SLNs

We performed *in vivo* experiments to investigate the controlled release behavior of H₂bdtc from H₂bdtc-SLNs; we also compared the activities of free H₂bdtc and H₂bdtc-SLNs against *T. cruzi*. We decided to use an H₂bdtc-SLNs concentration of 4 μmol kg⁻¹ day⁻¹. During the *in vivo* treatments on the basis of preliminary *in*

in vivo results obtained for the Y strain of *T. cruzi*, which revealed that H₂bdtc had low level of parasitemia (Supporting Information: Figure S1). In all the infected groups, parasitemia peaked at day 9 p.i., with gradual parasite elimination from the bloodstream after day 11 p.i. It is worth noting that we employed BZN concentrations 100 times lower than that used for Chagas patients. H₂bdtc-SLNs eliminated 70% of the circulating parasites at the peak of infection, whereas free H₂bdtc and the positive control BZN eliminated 48 and 15% of the parasites, respectively, as compared with the control group treated with PBS (Figure 4A). In agreement with the data revealing reduced parasitemia, mice treated with H₂bdtc-SLNs presented 100% survival rate (Figure 4B), similar to the result achieved with BZN administered at a clinical dose of 400 μmol kg⁻¹ day⁻¹ (100 times more concentrated than the concentration used herein). Compared with the control group (PBS), groups treated with free H₂bdtc and BZN exhibited a survival rate of 57%.

Cardiac and liver lesions

Encouraged by the *in vivo* results, we evaluated how free H₂bdtc, H₂bdtc-SLNs, and BZN affected the cardiac and hepatic tissues of the surviving animals. Infected mice treated with H₂bdtc-SLNs presented reduced cardiac inflammation (Figure 5A) and heart lesions were absent (Figure 5B), as established by the absence of CK-MB, the enzyme released into plasma during cardiac lesion.

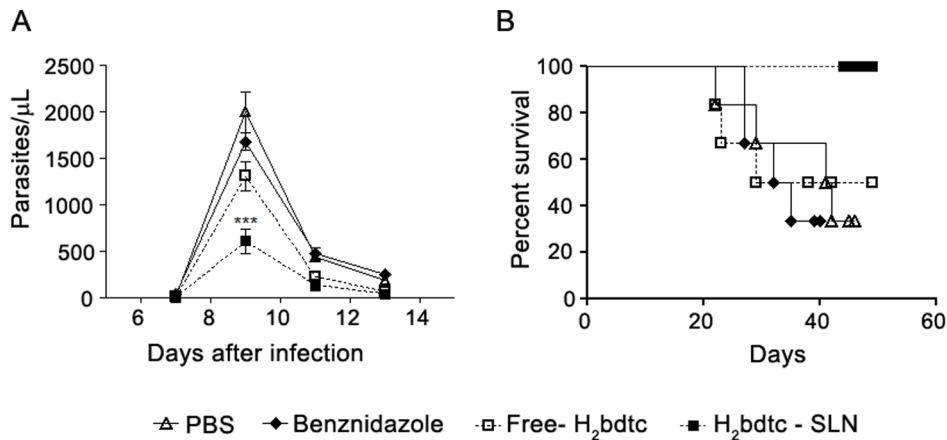


Figure 4. Parasitaemia and survival rates of mice infected with *T. cruzi* and treated with free H₂bdtc, H₂bdtc encapsulated in SLNs and BZN. (A) Parasitaemia was monitored on days 7, 9, 11 and 13 after infection. (B) Survival was monitored daily for 60 consecutive days. The mean + SEM is shown and is representative of three independent experiments (n = 7). Statistically significant differences compared with the control (BZN). T student test: ***p < 0.001
doi:10.1371/journal.pntd.0002847.g004

Treatment with free H₂bdtc diminished cardiac damage by 50% as compared with therapies with BZN or PBS. Concerning the ability of the tested compounds to reduce the liver damage caused

by the parasite, H₂bdtc-SLNs decreased inflammatory infiltration in the liver and hepatic toxicity more effectively, as assessed by measuring the glutamic-pyruvic transaminase (GTP) levels in the

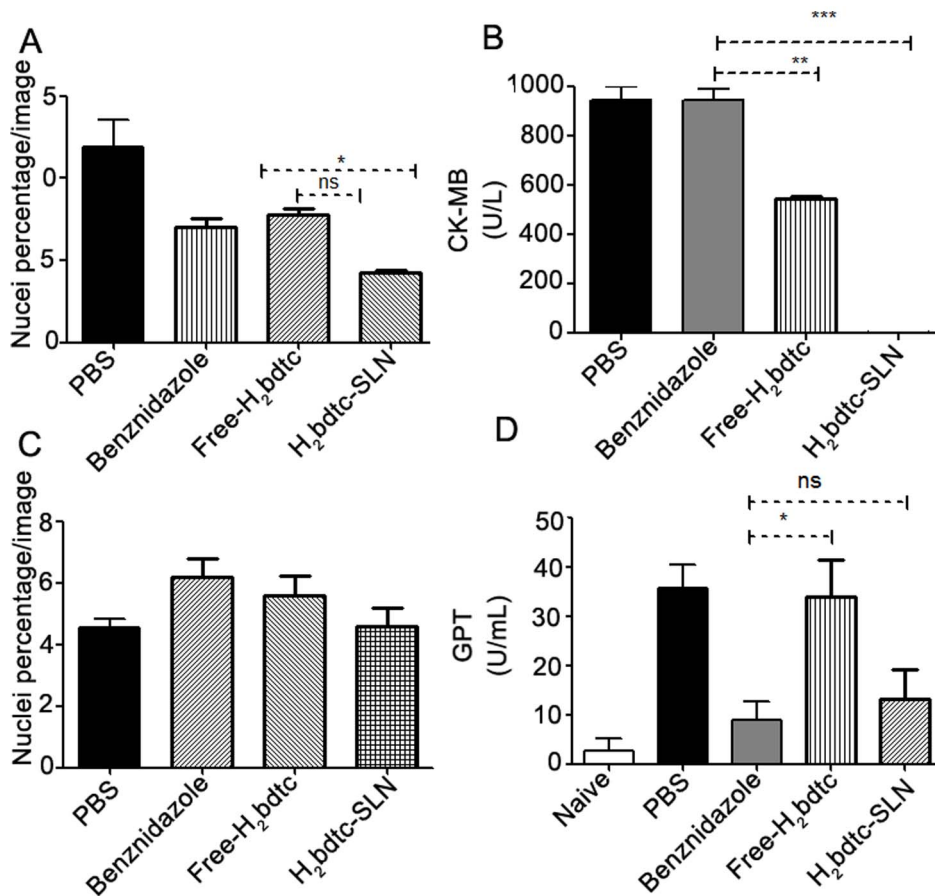


Figure 5. Cardiac and liver lesions of *T. cruzi*-infected animals after treatment with H₂bdtc encapsulated in solid lipid nanoparticles. (A) Quantification of cellular nuclei per 50 μm² of heart tissues derived from non-treated and treated animals. (B) Quantification of CK-MB in the serum of infected and treated mice. (C) Quantification of cellular nuclei per 50 μm² of liver tissues derived from non-treated and treated animals. (D) Quantification of glutamic-pyruvic transaminase (GPT) levels. The mean + statistically significant differences compared with the control are denoted by: *p < 0.05, **p < 0.01 e ***p < 0.001, T student test.
doi:10.1371/journal.pntd.0002847.g005

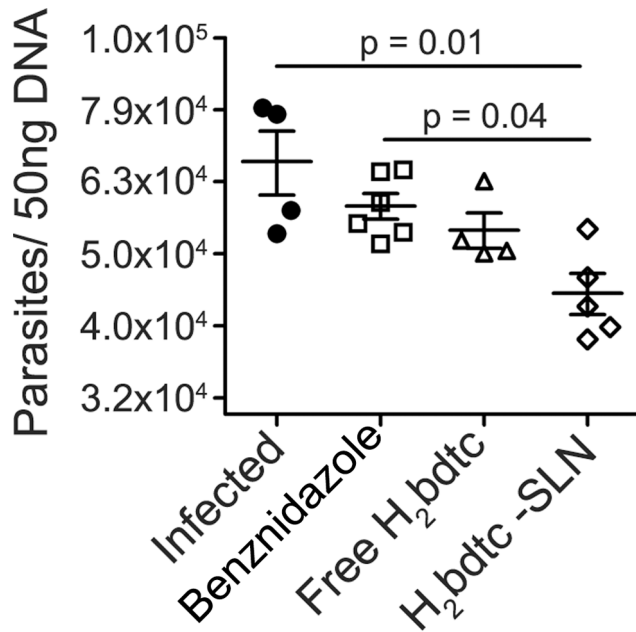


Figure 6. Quantification of the parasites load in cardiac tissues via real-time PCR. The presence of *T. cruzi* in infected heart tissue mice were analyzed by PCR 22days after infection. Statistically significant differences were showed in the figure. doi:10.1371/journal.pntd.0002847.g006

serum (Figure 5C, 5D). Considering all these results, it is possible to infer that treatment with H₂bdtc per se reduced exacerbation of the inflammatory response on *T. cruzi* target organs and, consequently, tissue damage. Loading of H₂bdtc into nanoparticles afforded even better results, producing no lesion in the heart tissue.

Because it is well established that parasites play an important role in cardiac damage during *T. cruzi* infection [42], [43], we quantified *T. cruzi* DNA derived from the heart tissues of mice treated with the tested compounds via real-time PCR. Treatment with H₂bdtc-SLNs reduced the parasite burden significantly more effectively as compared with the other tested drugs (Figure 6), indicating that killing the parasites is most likely the mechanism through which H₂bdtc-SLNs acts to diminish tissue lesions and enhance mice survival.

Discussion

Chagas disease has often been pointed out as being a major neglected disease; the drugs that are currently available to treat this disease are little effective [5], [12]. Efforts have been made to provide the affected populations with new compounds to treat the disease. In the past few years, researchers have tested many substances against *T. cruzi*. In particular, H₂bdtc, which belongs to the class of S-dithiocarbazates, is efficient against the parasite [21]. A 24-h UV-vis study into the stability of H₂bdtc in aqueous solution did not evidence any changes in the spectrum of this compound. Nevertheless, this drug is poorly soluble in water (1.50×10^{-6} M), which has limited its use to treat Chagas disease. Because H₂bdtc is lipophilic (Log $P_{(o/w)}$ = 2,69±0,03) and SLNs constitute effective oral drug delivery systems, we loaded H₂bdtc into this type of lipid.

We prepared the SLNs by the microemulsion method [31], [44], to avoid the use of organic solvents. The resulting SLNs had diameter of approximately 120 nm, dispersity lower than 0.3, and spherical shape, which made these lipids suitable for oral

administration [45], [46], [47], [48]. The zeta potential measurement allowed us to predict the stability of the colloidal dispersion. Charged particles have high zeta potential—negative or positive—and usually do not aggregate [49]. The zeta potential results revealed that the SNPs prepared here had a negative surface charge (-56.1 ± 4.4 mV), indicating that the system was physically stable. Loaded and unloaded SNPs had similar zeta potentials, attesting that the tested drug was completely and uniformly dispersed inside the lipid matrix [50].

Encapsulation did not change the *in vitro* trypanocidal activity of H₂bdtc, which was higher than the activity of BZN at the same concentration used here. The IC₅₀ values obtained for H₂bdtc against the trypomastigote form of the Y strain of *T. cruzi* were comparable with or superior to those of previously reported active compounds [51], [52]. Other papers have also described the use of colloidal drug carriers such as liposomes and nanoparticles to treat Chagas diseases [53], [54]. Treatment of *T. cruzi* infection with a BZN-loaded liposome increased BZN levels in the liver and blood. Intravenous administration of free BZN and BZN-encapsulated liposome at 0.2 mg of BZN per kilogram of body weight revealed three-fold higher BZN accumulation in the liver in the second case. Nevertheless, encapsulation failed to improve the *in vivo* BZN efficacy [55].

Liposome instability prevents their use as drug delivery systems [56]. Fortunately, we verified that free H₂bdtc and H₂bdtc-SLNs were not toxic to the spleen cells of Swiss mice, which encouraged us to directly test the effect of H₂bdtc formulations *in vivo* using a murine model of acute Chagas disease.

Treatment started with a relatively low oral dose of free H₂bdtc and H₂bdtc-SLNs ($4 \mu\text{mol kg}^{-1} \text{ day}^{-1}$) as compared with currently employed doses of the commercially available BZN and compounds tested in the literature [57], [58]. H₂bdtc-SLNs, Free H₂bdtc and BZN reduced the presence of parasites in the blood of infected mice in 70, 48 and 15% respectively. H₂bdtc-SLNs maintained 100% survival rate of infected mice, whereas 43% of the mice treated with free H₂bdtc or BZN at the same concentration succumbed to the disease. It is noteworthy that free SLN and PBS elicited similar levels of parasitemia (Supporting Information: Figure S2). Therefore, the use of SLNs as a drug delivery system increased the oral bioavailability of the target drug, as previously described [59], [60], [61], [62], [63]. H₂bdtc loading into SLNs overcame the problems inherent to the poor water solubility of the compound and may be could make it more accessible to the parasite (however, detailed pharmacokinetic data will be presented in a separate forthcoming paper). Additionally, some authors have proposed that drugs loaded into SLNs measuring 20–500 nm are absorbed by lymphatic transport, which reduces the first-pass metabolism [62], [63].

Analysis of histological sections of liver and heart tissues (Supporting Information: Figure: Figure S3 and Figure S4) revealed that the inflammatory infiltrate decreased in all the treated groups as compared with the control. The reduction was more pronounced in mice treated with H₂bdtc-SLNs, possibly because parasitemia was lower in this case. This corroborated with findings from previous studies [64], [65] and confirmed that the parasite elicited intense inflammation especially in the cardiac tissues. The fact that the heart tissues of mice treated with H₂bdtc-SLNs were perfectly preserved agreed with the notion that the presence of inflammatory infiltrates is associated with cardiac tissue damage [66], [67] and also with parasitic load [42], [43]. Indeed, mice treated with H₂bdtc-SLNs exhibited significantly lower parasite burden as compared with the other groups. Hence, the reduced parasitism elicited by H₂bdtc-SLNs helps to preserve the heart tissues of mice infected with *T. cruzi*, allowing us to conclude that H₂bdtc is a potent trypanocidal agent.

Investigation into how H₂bdtc interacts with possible targets represents a theme for future studies. For the time being, we must bear in mind that triazoles and thiosemicarbazones are well known for inhibiting cruzain, a protein belonging to the family of cysteine proteases and which is the most abundant protein in *T. cruzi*. Cruzain is essential for parasite development and survival within host cells [68]. H₂bdtc bears pyrazole and dithiocarbamate parts, which are similar to triazoles and thiosemicarbazones, respectively, and could account for its trypanocidal action.

A mechanism of action similar to that of BZN probably does not occur. The BZN mode of action involves intracellular reduction of the nitro group, to produce highly reactive free radicals and/or electrophilic metabolites that could affect other systems, especially host systems, contributing to the cytotoxic effects observed in BZN-treated patients [69].

It is worth noting that cysteine proteases are very important for parasites; however, the lack of redundancy with respect to their mammalian hosts makes these proteases interesting targets for the development of new therapeutic agents [70]. Altogether, our findings show that H₂bdtc-SLN is a possible drug candidate to treat Chagas disease: it is more efficient against *T. cruzi* than the drugs used in current therapies.

Supporting Information

Figure S1 *In vivo* evaluations of the trypanocidal activity free-H₂bdtc and H₂bdtc-SLN (concentrations 4 μM, 40 μM and 80 μM) (—) Parasitaemia rate of mice infected with *T. cruzi* and treated with free-H₂bdtc. (---) Parasitaemia rate of mice infected with *T. cruzi* and treated with H₂bdtc encapsulated in solid lipid nanoparticles. Parasitaemia was monitored on days 7, 9, 11 and 13 after infection. The mean + SEM is shown and is representative of three independent

experiments (n = 7). Statistically significant differences compared with the free-H₂bdtc. T student test: **p<0.01 and ***p<0.001.

(TIF)

Figure S2 Parasitaemia of mice infected with *T. cruzi* and treated with free SLNs and PBS. Parasitaemia was monitored on days 7, 9, 11 and 13 after infection.

(TIF)

Figure S3 Cardiac lesions of *T. cruzi*-infected animals after treatment with H₂bdtc encapsulated in SLNs. The sections represent of heart tissues inflammatory process composed of various cell types (21 days after infection).

(TIF)

Figure S4 Liver lesions of *T. cruzi*-infected animals after treatment with H₂bdtc encapsulated in SLNs. The sections represent of liver tissues inflammatory process composed of various cell types (21 days after infection).

(TIF)

Acknowledgments

We give special thanks to Dr. Denise Brufato Ferraz and Professor Roberto S. da Silva for their technical support.

Author Contributions

Conceived and designed the experiments: ZAC PIdSM RSC CDL TAP CMM MAPdS RFVL JSS VMD. Performed the experiments: ZAC PIdSM RSC CDL TAP CMM MAPdS. Analyzed the data: ZAC PIdSM RSC CDL TAP CMM MAPdS RFVL JSS VMD. Contributed reagents/materials/analysis tools: ZAC PIdSM TAP MAPdS RFVL VMD JSS. Wrote the paper: ZAC PIdSM TAP.

References

- Lountos GT, Tropea JE, Waugh DS (2013) Structure of the Trypanosoma cruzi protein tyrosine phosphatase TcPTP1, a potential therapeutic target for Chagas' disease. *Molecular and Biochemical Parasitology* 187: 1–8. doi:10.1016/j.molbiopara.2012.10.006.
- Coura JR, Vinas PA (2010) Chagas disease: a new worldwide challenge. *Nature* 465: S6–S7.
- Clayton J (2010) Chagas disease 101. *Nature* 465: S4–S5.
- Petherick A, Ventura-Garcia L, Roura M, Pell C, Posada E (2013) Socio-Cultural Aspects of Chagas Disease: A Systematic Review of Qualitative Research. *PLoS Negl Trop Dis* 7: e2410. doi:10.1371/journal.pntd.0002410.t002.
- Reidpath D, Allotey P, Pokhrel S (2011) Social sciences research in neglected tropical diseases 2: A bibliographic analysis. *Health Res Policy and Systems* 9: 1 doi:10.1186/1478-4505-9-1.
- World Health Organization (2010) First WHO report on neglected tropical diseases. Available: http://www.who.int/neglected_diseases/2010report/en/. Accessed in 23 August 2013.
- Guedes PM, Silva GK, Gutierrez FR, Silva JS (2011) Current status of Chagas disease chemotherapy. *Expert Rev Anti-infective Therapy* 9: 609–620. doi: 10.1586/eri.11.31.
- Urbina JA (2010) Specific chemotherapy of Chagas disease: relevance, current limitations and new approaches. *Acta Trop* 115: 55–68. doi: 10.1016/j.actatropica.2009.10.023.
- Murcia L, Carrilero B, Segovia M (2012) Limitations of currently available Chagas disease chemotherapy. *Rev Española de Quimioterapia* 25: 1–3.
- Viotti R, Alarcón de Noya B, Araujo-Jorge T, Grijalva MJ, Guhl F, López MC, Ramsey JM, Ribeiro I, Schijman AG, Sosa-Estani S, Torrico F, Gascon J (2013) Towards a Paradigm Shift in the Treatment of Chronic Chagas Disease. *Antimicrobial Agents and Chemotherapy* 58: 263–269. doi: 10.1128/AAC.01662-13.
- Selzer PM (2013) Trypanosomatid Diseases: Molecular Routes to Drug Discovery, Drug Discovery in Infectious Diseases: European Cooperation in Science and Technology 450 p.
- Castro A, Meca MM, Bartel LC (2006) Toxic Side Effects of Drugs Used to Treat Chagas Disease (American Trypanosomiasis). *Human Exp Toxicol* 25: 471–479. doi: 10.1191/0960327106het653oa.
- Altchek J, Moscatelli G, Moroni S, Garcia-Bourmissen F, Freilij H (2011) Adverse Events After the Use of Benzimidazole in Infants and Children With Chagas Disease. *Pediatrics* 127: e212–e218. doi: 10.1542/peds.2010-1172.
- Abad-Franch F, Diotaiuti L, Gurgel-Gonçalves R, Gürtler R E (2013) Certifying the interruption of Chagas disease transmission by native vectors: cui bono? *Mem. Inst. Oswaldo Cruz* 108: 251–254.
- Guedes PMM, Gutierrez FRS, Nascimento MSL, Do-Valle-Matta MA, Silva JS (2012) Antiparasitai chemotherapy in Chagas' disease cardiomyopathy: current evidence. *Trop Med and Int Health* 17: 1057–1065. doi: 10.1111/j.1365-3156.2012.03025.x.
- Beshir AB, Guchhai SK, Gascón JA, Fenteany G (2008) Synthesis and structure–activity relationships of metal–ligand complexes that potently inhibit cell migration. *Bioorg Med Chem Lett* 18: 498–504. doi: 10.1016/j.bmcl.2007.11.099
- Tarafter MTH, Jin KT, Crouse KA, Ali AM, Yamin BM, et al. (2002) Coordination chemistry and bioactivity of Ni²⁺, Cu²⁺, Cd²⁺ and Zn²⁺ complexes containing bidentate Schiff bases derived from S-benzylthiocarbamate and the X-ray crystal structure of bis[S-benzyl-β-N-(5-methyl-2-furylmethylene) dithiocarbamate] cadmium (II). *Polyhedron* 21: 2547–2554.
- Pavan FR, Maia PIS, Leite SRA, Deflon VM, Batista AA, et al. (2010) Thiosemicarbazones, semicarbazones, dithiocarbazates and hydrazide/hydrazones: Anti – Mycobacterium tuberculosis activity and cytotoxicity. *Eur J Med Chem* 45: 1898–1905. doi: 10.1016/j.ejmech.2010.01.028
- Maurya MR, Kumar A, Bhat AR, Azam A, Bader C, et al. (2006) Dioxo- and Oxovanadium(V) Complexes of Thiohydrazone ONS Donor Ligands: Synthesis, Characterization, Reactivity, and Antiamoebic Activity. *J Inorg Chem* 45: 1260–1269. doi: 10.1021/ic050811
- Tampouris K, Coco S, Yannopoulos A, Koinis S (2007) Palladium(II) complexes with S-benzyl dithiocarbamate and S-benzyl-N-isopropylidenedithiocarbamate: Synthesis, spectroscopic properties and X-ray crystal structures. *Polyhedron* 26: 4269–4275. doi: 10.1016/j.poly.2007.05.039.
- Maia PIS, Fernandes AGA, Silva JJJN, Andricopulo AD, Lemos SS, et al. (2010) Dithiocarbamate complexes with the [M(PPh₃)₂]⁺ (M = Pd or Pt) moiety: Synthesis, characterization and anti-Trypanosoma cruzi activity. *J Inorg Biochem* 104: 1276–1282. doi:10.1016/j.jinorgbio.2010.08.009.
- Silva AC, Kumar A, Wild W, Ferreira D, Santos D, et al. (2012) Long-term stability, biocompatibility and oral delivery potential of Risperidone-loaded solid nanoparticles. *Int J Pharm* 15: 798–805. doi: 10.1016/j.ijpharm.2012.07.058
- Chakraborty S, Shukla D, Mishra B, Singh S (2009) Lipid: an emerging platform for oral delivery of drugs with poor bioavailability. *Eur J Pharm and Biopharm* 75: 1–15. doi: 10.1016/j.ejpb.2009.06.001

24. Muller RH, Mehnert W., Lucks JS, Schwarz C, Zur Muhlen A, et al. (1995) Solid lipid nanoparticles (SLNs) – an alternative colloidal carrier system for controlled drug delivery. *Eur J Pharm and Biopharm* 41: 62–69.
25. Muller RH, Radtke M, Wissing SA (2002) Solid lipid nanoparticles (SLNs) and nanostructured lipid carriers (NLC) in cosmetic and dermatological preparations. *Adv Drug Delivery Revs* 54: 131–155. doi: 10.1016/S0169-409X(02)00118-7.
26. Taveira SF, Araujo LMPC, de Santana DCAS, Nomizo A, Freitas LAP, Lopez RFV (2012) Development of Cationic Solid Lipid Nanoparticles with Factorial Design-Based Studies for Topical Administration of Doxorubicin. *J Biomed Nanotechnol* 8: 219–228. doi: 10.1166/jbn.2012.1383.
27. Morales-Neto R, Hulshof L, Ferreira CV, Gadelha FR (2009) Distinct Phosphatase Activity Profiles in Two Strains of *Trypanosoma cruzi*. *Journal of Parasitology* 95: 1525–1531. doi:10.1645/GE-1899.1
28. Buscaglia CA, Di Noia JM (2003) *Trypanosoma cruzi* clonal diversity and the epidemiology of Chagas' disease. *Microbes and Infection* 5: 419–427. doi: 10.1016/S1286-4579(03)00050-9
29. Ekambaram P, Sathali Aah, Priyanka K (2012) Solid Lipid Nanoparticles: A Review. *Sciences Reviews Chemical Communication* 2: 80–102
30. Salomon CJ (2012) First century of chagas' disease: An overview on novel approaches to nifurtimox and benznidazole delivery systems. *J Pharm Sci* 101: 888–894. DOI: 10.1002/jps.23010
31. Marquê-Oliveira F, Santana DCA, Taveira SAF, Vermeulen DM, Oliveira ARM, et al. (2010) Development of nitrosyl ruthenium complex-loaded lipid carriers for topical administration: improvement in skin stability and in nitric oxide release by visible light irradiation. *J Pharm and Biom Anal* 53: 843–851. doi:10.1016/j.jpba.2010.06.007.
32. Kovačević AB, Müller RH, Savić SD, Vuleta GM, Keck CM. (2014) Solid lipid nanoparticles (SLN) stabilized with polyhydroxy surfactants: Preparation, characterization and physical stability investigation. *Colloids and Surfaces A: Physicochem. Eng. Aspects* 444:15–25. doi: 10.1016/j.colsurf.2013.12.023
33. Potta SG, Minemi S, Nukala RK, Peinado C, Lamprou DA, et al. (2011) Preparation and characterization of ibuprofen solid lipid nanoparticles with enhanced solubility. *J Microencapsulation* 28: 47–81. doi:10.3109/02652048.2010.529948.
34. Bhalekar MR, Pokharkar V, Madgulkar A, Patil N, Patil N (2009) Preparation and Evaluation of Miconazole Nitrate-Loaded Solid Lipid Nanoparticles for Topical Delivery. *AAPS PharmSciTech* 10: 289–296. Doi: 10.1208/s12249-009-9199-0.
35. Lopes RF, Collett JH, Bentley MV (2000) Influence of cyclodextrin complexation on the in vitro permeation and skin metabolism of dexamethasone. *Int J Pharm* 200: 127–132. doi: 10.1016/S0378-5173(00)00365-3
36. Silva JJ, Osakabe AL, Pavanelli WR, Silva JS, Franco DW (2007). *In vitro* and *in vivo* antiproliferative and trypanocidal activities of ruthenium NO donors. *Br J Pharmacol* 152 (1): 112–121.
37. Brener Z (1962) Therapeutic activity and criterion of cure on mice experimentally infected with *Trypanosoma cruzi*. *Rev Inst Med Trop* 4: 389–396.
38. Brener Z (1962a) Observations on immunity to superinfections in mice experimentally inoculated with *Trypanosoma cruzi* and subjected to treatment. *Rev Inst Med Trop* 4: 119–123.
39. Cummings KL, Tarleton RL (2003) Rapid quantitation of *Trypanosoma cruzi* in host tissue by real-time PCR. *Mol Biochem Parasitol* 129: 53–59. doi: 10.1016/S0166-6851(03)00093-8
40. Maekawa M, Sugiura A, Iwahara K, Sakai Y, Kishi K (2012) Effect of the Inhibition of mitochondrial Creatine Kinase Activity on the Clinical Diagnosis of Suspected Acute Myocardial Infarction. *The Open Clin Chem J* 5: 1–6.
41. Reitman S, Frankel S (1957) Glutamic – pyruvate transaminase assay by colorimetric method. *Am J Clin Pathol* 28: 56–63.
42. Borges DC, Araujo NM, Cardoso CR, Chica JEL (2012) Different parasite inocula determine the modulation of the immune response and outcome of experimental *Trypanosoma cruzi* infection. *Immunology* 138: 145–156. doi: 10.1111/imm.12022.
43. Corral RS, Guerrero NA, Cuervo H, Gironès N, Fresno M (2013) *Trypanosoma cruzi* Infection and Endothelin-1 Cooperatively Activate Pathogenic Inflammatory Pathways in Cardiomyocytes. *PLoS Negl Trop Dis* 7: e2034. doi:10.1371/journal.pntd.0002034.
44. Zhang Z, Bu H, Gao Z, Huang Y, Gao F, et al. (2010) The characteristics and mechanism of simvastatin loaded lipid nanoparticles to increase oral bioavailability in rats. *Int J Pharm* 394: 147–153. doi: 10.1016/j.ijpharm.2010.04.039.
45. Li H, Zhao X, Ma Y, Zhai G, Li L, Lou H (2009) Enhancement of gastrointestinal absorption of quercetin by solid lipid nanoparticles. *J Controlled Release* 133: 238–244. doi: 10.1016/j.jconrel.2008.10.002.
46. Mehwert W, Mader K (2012) Solid lipid nanoparticles: production, characterization and applications. *Adv drug delivery revs* 64: 83–101. doi: 10.1016/S0169-409X(01)00105-3.
47. Gasco MR (1993) Method for producing solid lipid nanospheres have a narrow size distribution. US Patent 5: 250–236.
48. Chen CC, Tsai TH, Huang ZR, Fang JY (2010) Effects of lipophilic emulsifier on the oral administration of lovastatin from nanostructured lipid carriers: Physicochemical characterization and pharmacokinetics. *Eur J Pharm and Biopharm* 74: 474–482. doi:10.1016/j.ejpb.2009.12.008.
49. Monshi A, Salehi R, Fathi MH, Karbasi S, Pieleś U, Daniels AU (2012) Preparation, chemistry and physical properties of bone-derived hydroxyapatite particles having a negative zeta potential. *Mater Chem Phys* 132: 446–452. doi:10.1016/j.matchemphys.2011.11.051
50. Varshosaz J, Eskandari S, Tabbakhian M (2012) Freeze - drying of nanostructure lipid carriers by different carbohydrate polymers used as cryoprotectants. *Carbohydr Polym* 88: 1157–1163. doi: 10.1016/j.carbpol.2012.01.051.
51. Moreira DRM, Costa SPM, Hernandez MZ, Rabello MM, Filho GBO (2012) Structural Investigation of Anti-*Trypanosoma cruzi* 2-Iminothiazolidin-4-ones Allows the Identification of agents with Efficacy in Infected Mice. *Med Chem Res* 55: 10918–10936. doi: 10.1021/jm301518v.
52. Caputto ME, Ciccarelli A, Frank F, Moglionia AG, Moltrasio GY (2012) Synthesis and biological evaluation of some novel 1-indanone thiazolyldiazone derivatives as anti-*Trypanosoma cruzi* agents. *Eur J Med Chem* 55: 155–163. doi: 10.1016/j.ejmech.2012.07.013.
53. González-Martin G, Merino I, Rodríguez-Cabezas M, Torres M, Nuñez R, (1998) Characterization and tripanocidal activity of nifurtimox-containing and empty nanoparticles of polyethylcyanoacrylates. *J Pharm and Pharmacol* 50: 29–35.
54. Sánchez G, Cuellar D, Zulantay I, Gajardo M, González-Martin G (2002) Cytotoxicity and trypanocidal activity of nifurtimox encapsulated in ethylcyanoacrylate nanoparticles. *Biol Res* 35: 39–45.
55. Morilla MJ, Montanari JA, Prieto MJ, Lopez MO, Petray PB (2004) Intravenous liposomal BZN as trypanocidal agent: increasing drug delivery to liver is not enough. *Int J Pharm* 8: 8278–280. doi: 10.1016/j.ijpharm.2004.03.025.
56. Date AA, Joshi MD, Patravale VB (2007) Parasitic diseases: Liposomes and polymeric nanoparticles versus lipid nanoparticles. *Advanced drug delivery reviews* 59: 505–521. doi: 10.1016/j.addr.2007.04.009.
57. Coura JR (2009) Present situation and new strategies for Chagas disease chemotherapy - a proposal. *Mem Inst Oswaldo Cruz* 104: 549–554. doi: 10.1590/S0074-02762009000400002.
58. Zhu X, Liu Q, Yang S, Parman T, Green CE (2012) Evaluation of Arylimidamides DB1955 and DB1960 as Candidates against Visceral Leishmaniasis and Chagas' Disease: *In Vivo* Efficacy, Acute Toxicity, Pharmacokinetics, and Toxicology Studies. *Antimicrob agents and chemother* 56: 3690–3699. doi: 10.1128/AAC.06404-11.
59. Burra M, Jukanti R, Janga KY, Sunkavali S, Velpula A (2013) Enhanced intestinal absorption and bioavailability of raloxifene hydrochloride via lyophilized solid lipid nanoparticles. *Adv powder technol* 24: 393–402. doi:10.1016/j.apt.2012.09.002.
60. Singh A, Ahmad I, Akhter S, Jain GK, Iqbal Z (2013) Nanocarriers based formulation of Thymoquinone improves oral delivery: stability assessment, *in vitro* and *in vivo* studies. *Colloids and Surfaces B: Biointerfaces* 102: 822–832. doi:10.1016/j.colsurf.2012.08.038.
61. Chalikwar SS, Belgamwar VS, Talele VR, Surana SJ, Patil MU (2012) Formulation and evaluation of Nimmodipine-loaded solid lipid nanoparticles delivered via lymphatic transport system. *Colloids and Surfaces B: Biointerfaces* 97: 109–116. doi:10.1016/j.colsurf.2012.04.027.
62. Venishetty VK, Chede R, Komuravelli R, Adepu L, Sistla R (2012) Design and evaluation of polymer coated carvedilol loaded solid lipid nanoparticles to improve the oral bioavailability: a novel strategy to avoid intraduodenal administration. *Colloids and Surfaces B: Biointerfaces* 95: 1–9. doi:10.1016/j.colsurf.2012.01.001.
63. Tiwari R, Pathak K (2011) Nanostructured lipid carriers versus solid lipid nanoparticles of simvastatin: comparative analysis of characteristics, pharmacokinetics and tissue uptake. *Int J Pharmacol* 415: 232–243. doi: 10.1016/j.ijpharm.2011.05.044.
64. Machado MPR, Rocha AM, Oliveira LF, Cuba MB, Loss LO (2012) Autonomic nervous system modulation affects the inflammatory immune response in mice with acute Chagas disease. *Exp Physiol* 97: 1186–1202. doi: 10.1113/expphysiol.2012.066431.
65. Torrecilhas ACT, Tonelli RR, Pavanelli WR, Silva JS, Schumacher RI, (2009) *Trypanosoma cruzi*: parasite shed vesicles increase heart parasitism and generate an intense inflammatory response. *Microbes Infect* 11: 29–39. doi:10.1016/j.micinf.2008.10.003.
66. Bonney KM, Gifford KM, Taylor JM, Chen CI, Engman DM (2013) Cardiac damage induced by immunization with heat-killed *Trypanosoma cruzi* is not antibody mediated. *Parasite Immunol* 35: 1–10. doi: 10.1111/pim.12008.
67. Berrios AM, Estrada CC, Lapier M, Duaso J, Kemmerling U (2013) BZN prevents endothelial damage in experimental model of Chagas disease. *Acta Trop* 127: 6–13. doi: 10.1016/j.actatropica.2013.03.006.
68. Dias LC, Dessoy MA, Silva JN, Thiemann OH, Oliva G (2009) Chemotherapy of Chagas' disease: state of the art and perspectives for the development of new drugs. *Quim Nova* 32: 2444–2457. doi:10.1590/S0100-40422009000900038.
69. Castro JA, Mecca MM, Bartel LC (2006) Toxic side effects of drugs used to treat Chagas' disease (American trypanosomiasis). *Human Exp Toxicol* 25: 471–479.
70. Chena YT, Liraa R, Hansell E, McKerrow JH, Rousa WR (2008) Synthesis of macrocyclic trypanosomal cysteine protease inhibitors. *Bioorg Med Chem Lett* 18: 5860–5863. doi:10.1016/j.bmcl.2008.06.012.